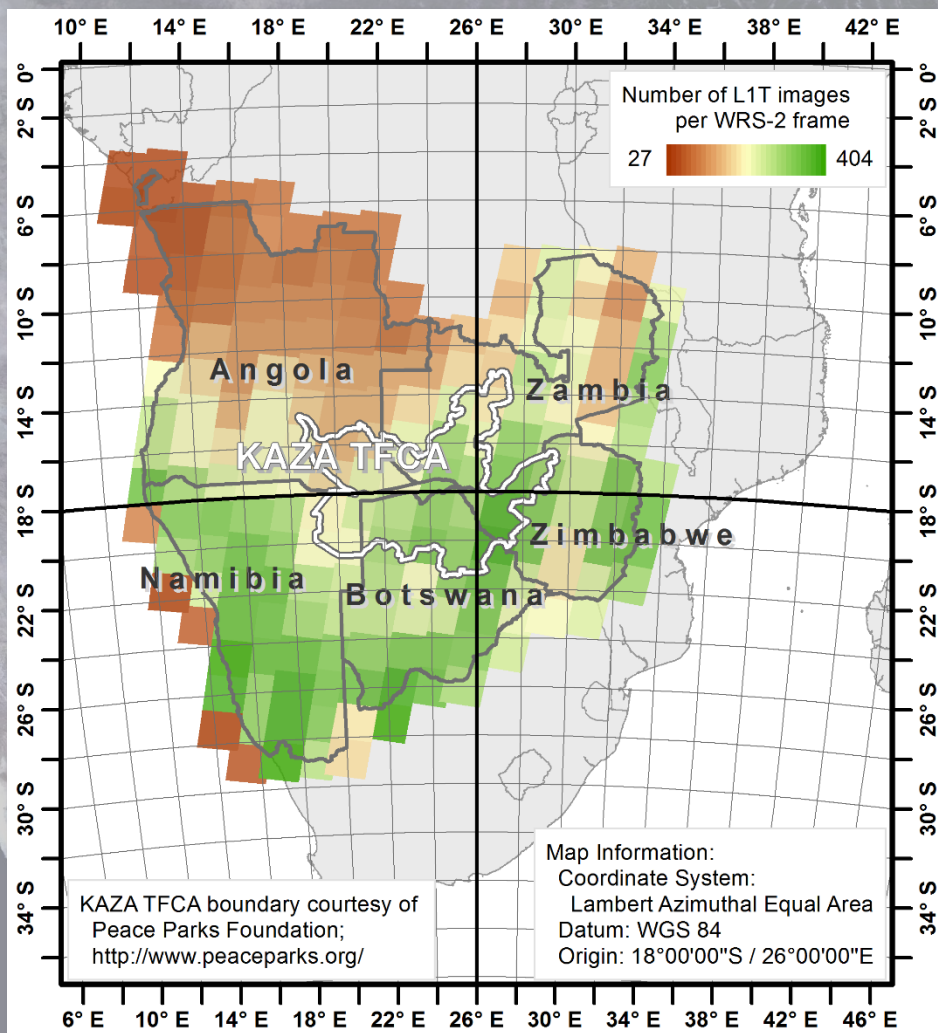


Generating phenology-adaptive pixel-based Landsat composites across large areas

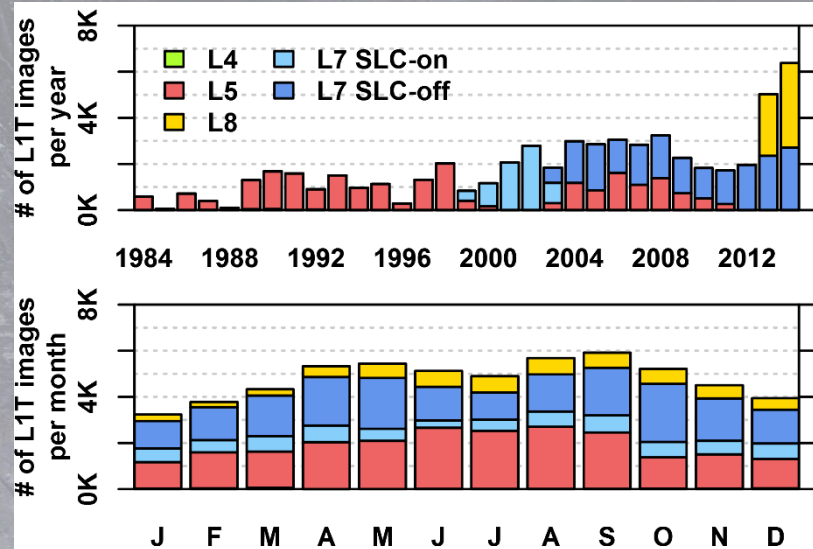
4. Gemeinsame Jahrestagung der Arbeitskreise Fernerkundung
Daten – Informationen – Entscheidungen
24./25. Sept. 2015, Geozentrum der Universität Bonn

David Frantz, Achim Röder, Marion Stellmes, Joachim Hill
Department of Environmental Remote Sensing & Geoinformatics,
FB VI Regional and Environmental Sciences, Trier University

Centered at the upcoming Kavango-Zambezi Transfrontier Conservation Area (KAZA TFCA)



- ~ 3.7 Mio. km²
- 57,371 L1T images
- 194 footprints
- ~ 15 TB



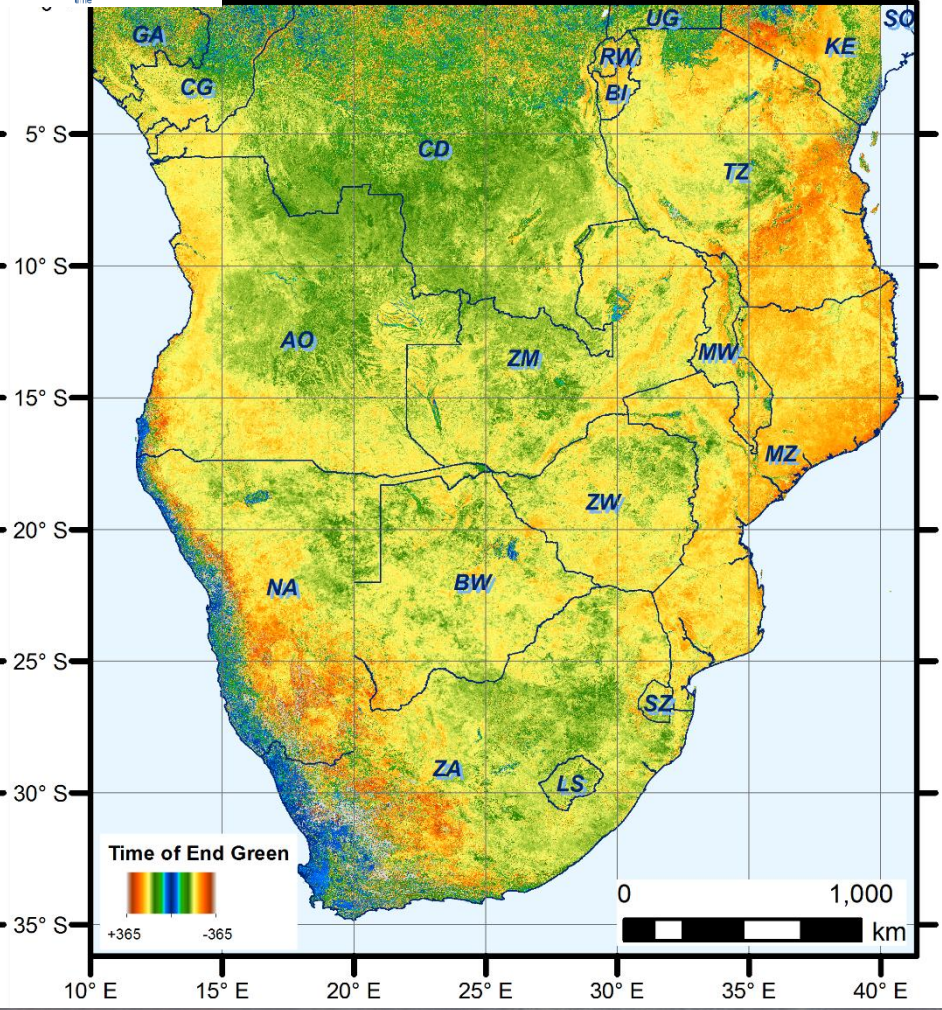
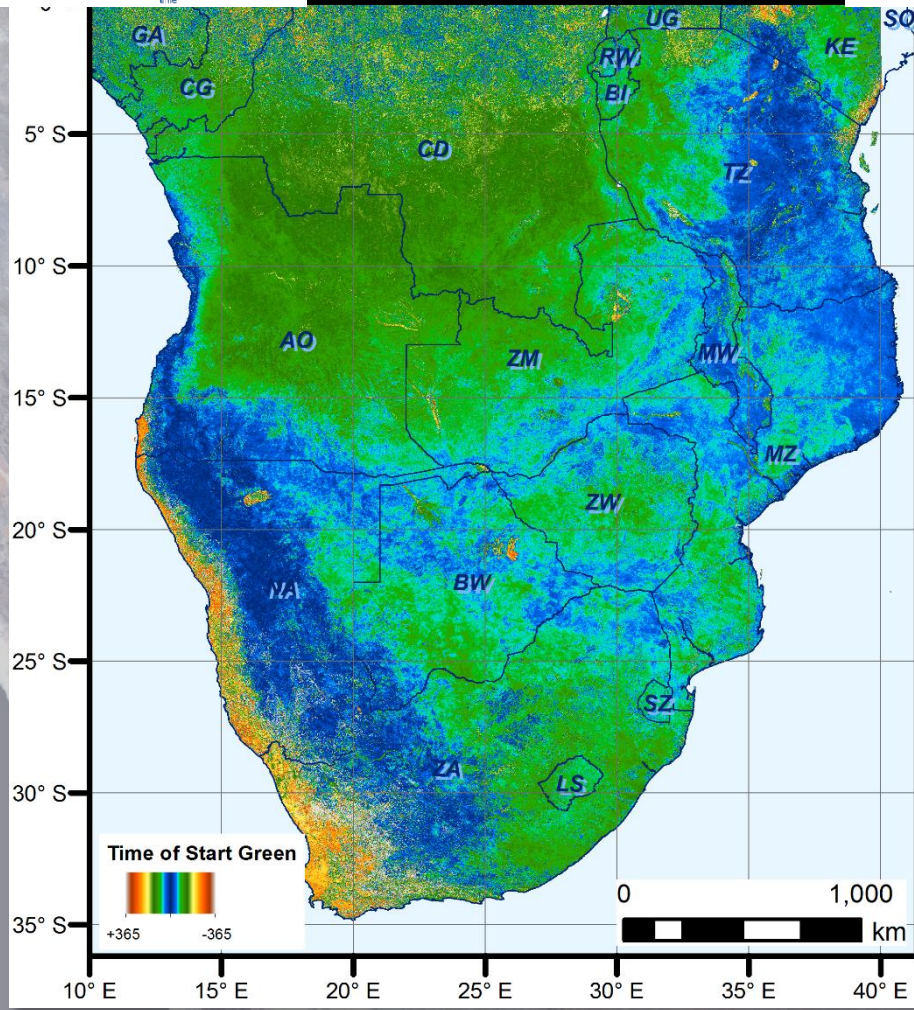
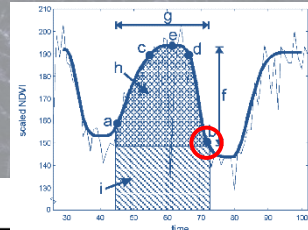
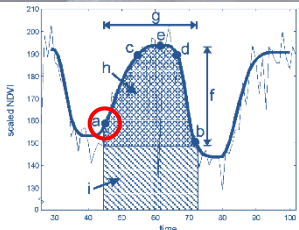
➔ **wall-to-wall applications**

- e.g. forest cover + change/trend: deforestation/degradation
- Biophysical parameters: stand structure, tree height, biomass, ...

➔ **pixel-based composites**

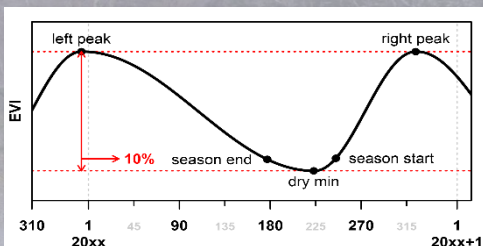
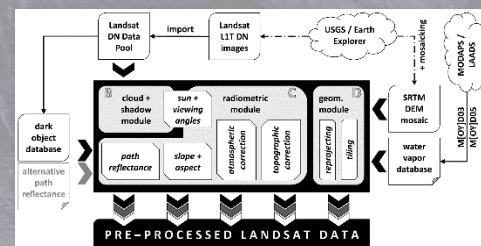
state-of-the art: static target DOY

Study Area / Motivation



LANDSAT PRE-PROCESSING

- cloud masking
- radiometric correction
- gridded data structure

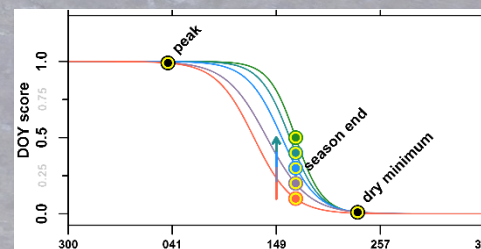


LAND SURFACE PHENOLOGY

- MODIS phenology
- Data fusion by spatial unmixing → medium resolution phenology

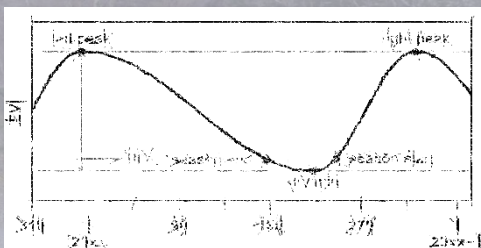
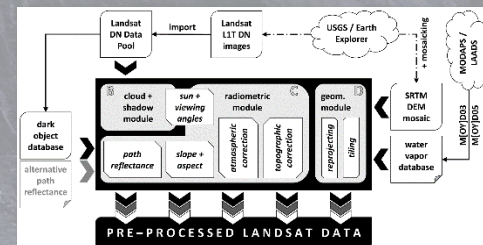
PIXEL-BASED COMPOSITES

- Generation of seamless large area baseline reflectance data
- Compositing guided by phenology



LANDSAT PRE-PROCESSING

- cloud masking
- radiometric correction
- gridded data structure

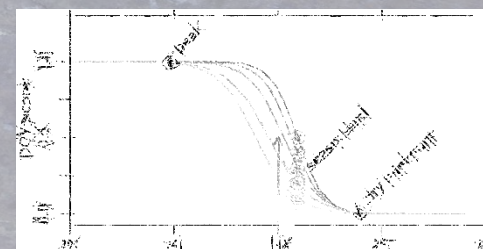


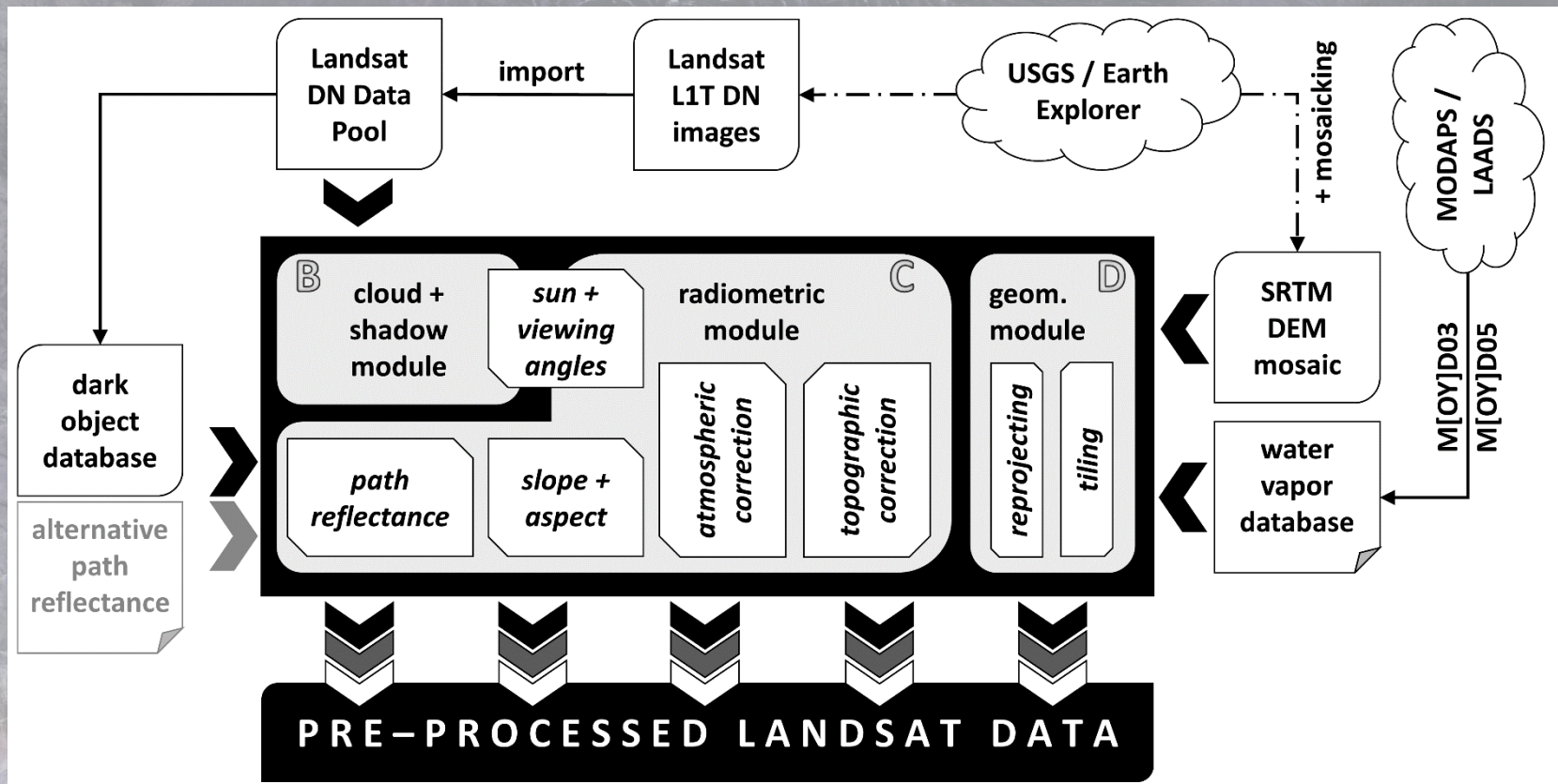
LAND SURFACE PHENOLOGY

- MODIS phenology
- Data fusion by spatial unmixing → medium resolution phenology

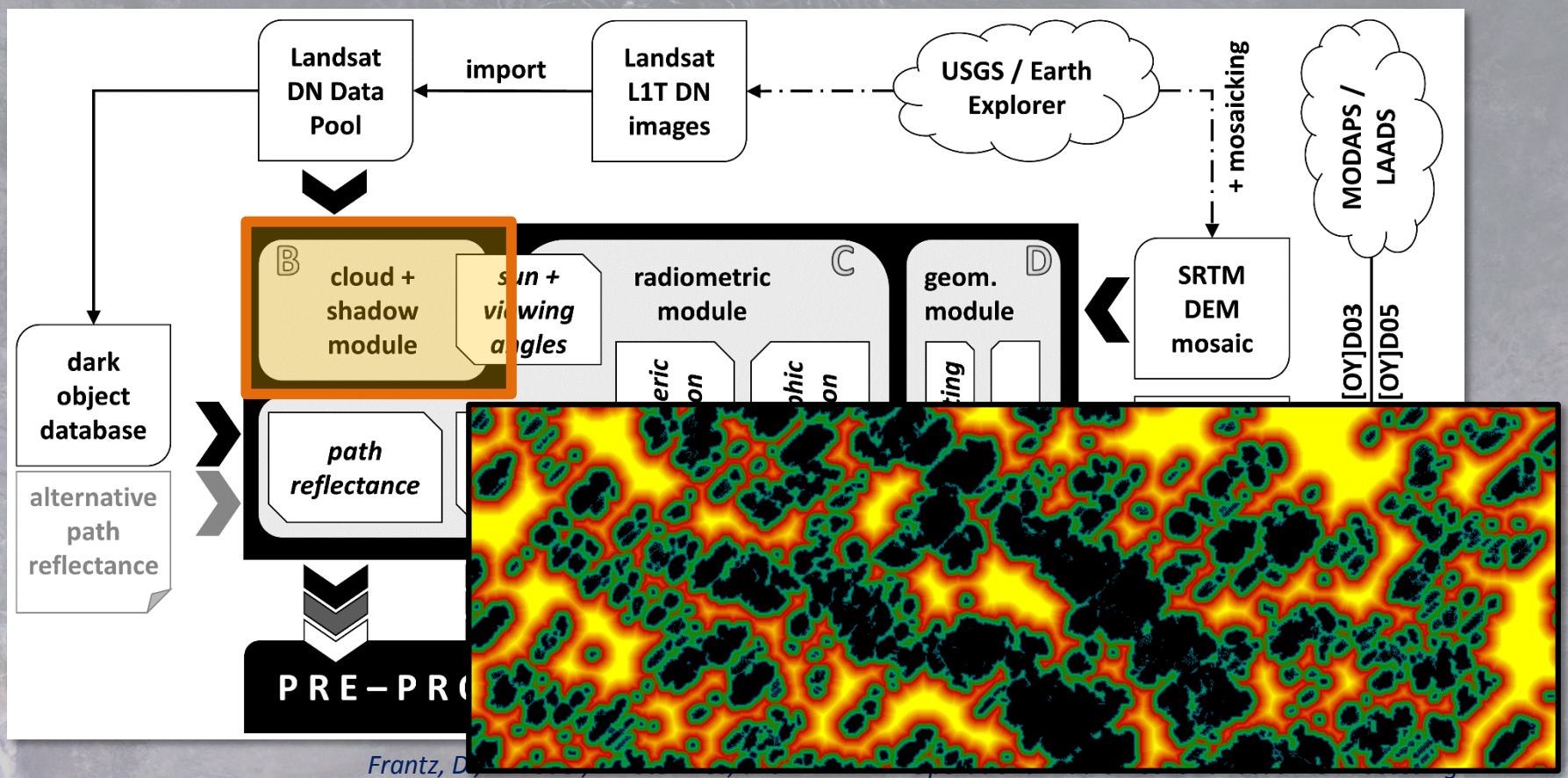
PIXEL-BASED COMPOSITES

- Generation of seamless large area baseline reflectance data
- Compositing guided by phenology





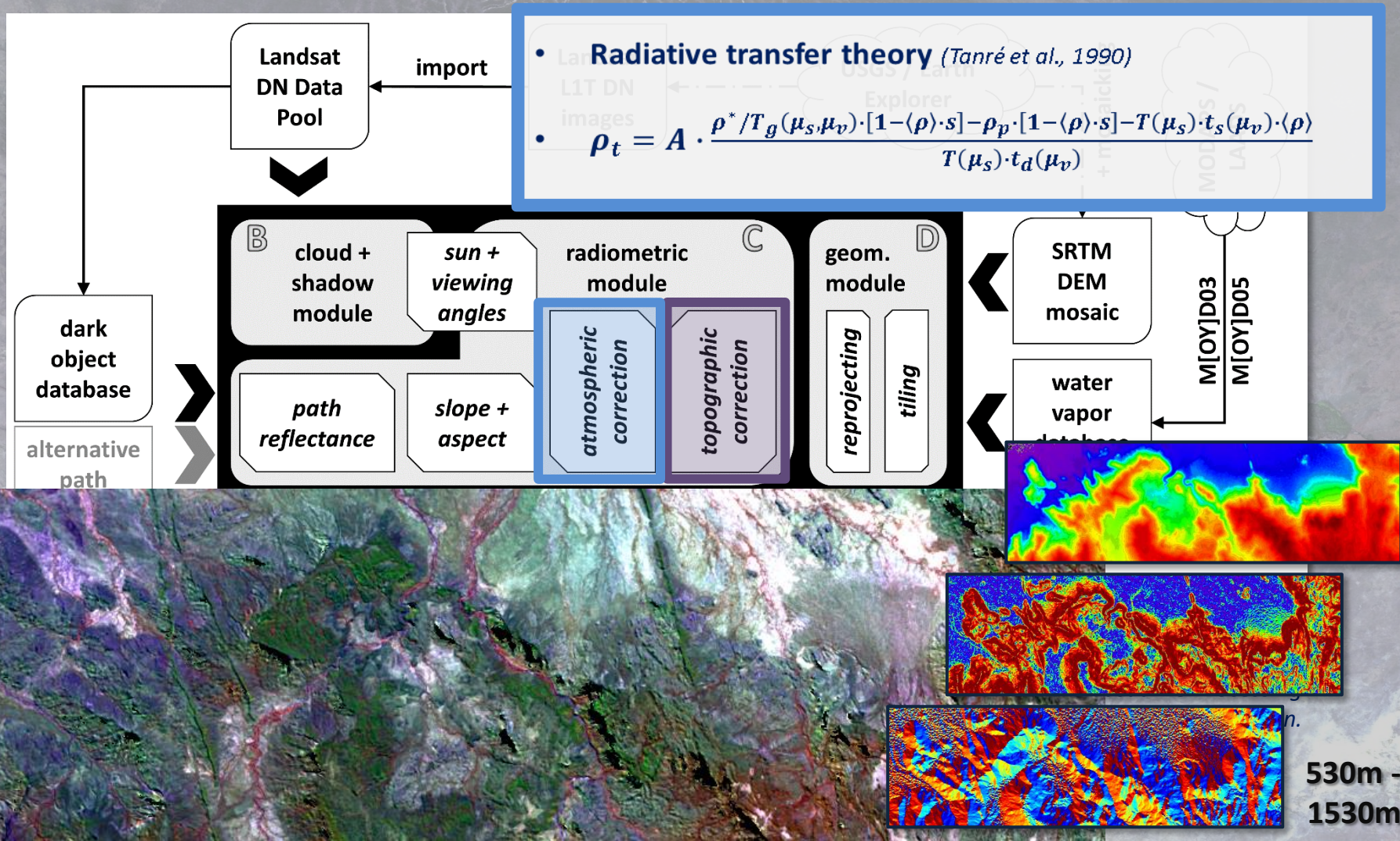
Frantz, D., A. Röder, M. Stellmes, and J. Hill. "An Operational Radiometric Landsat Pre-Processing Framework for Large Area Time Series Applications." In Revision.

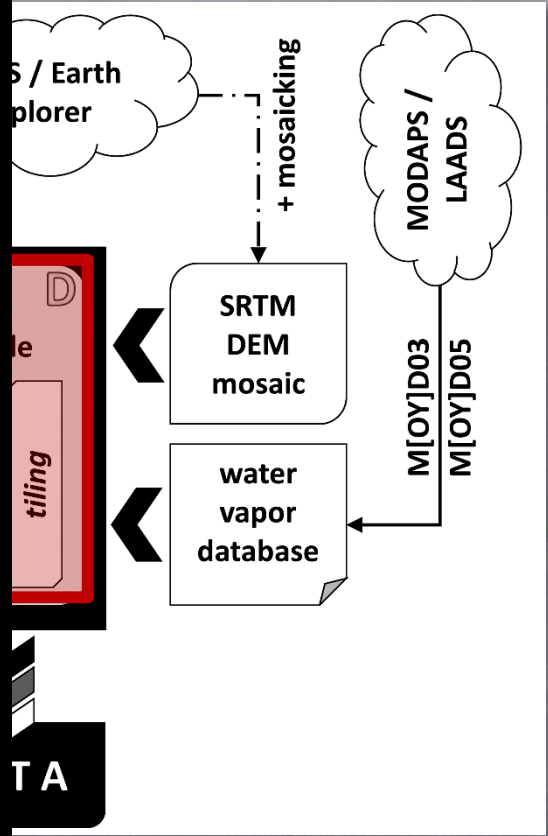
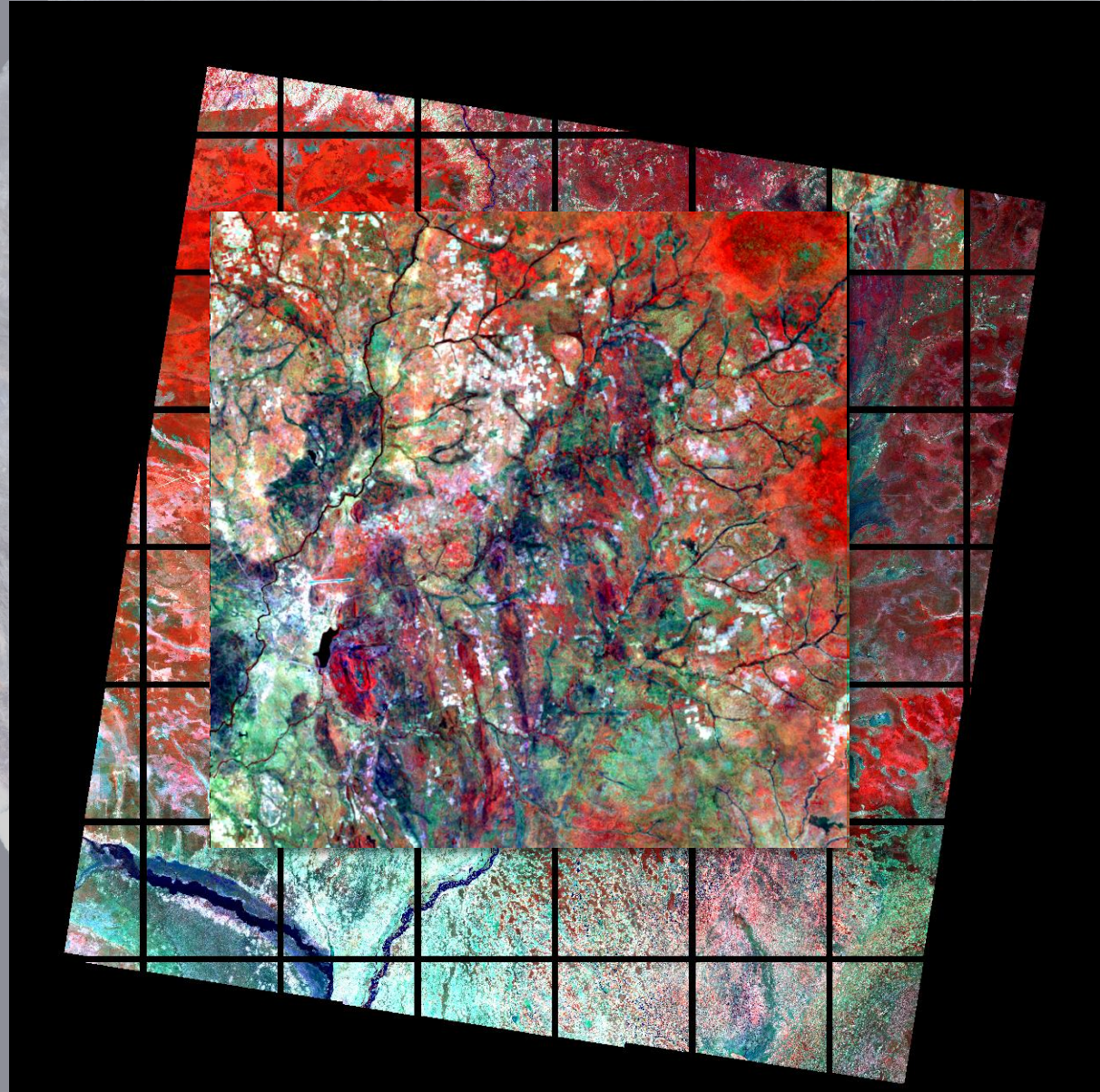


Frantz, D

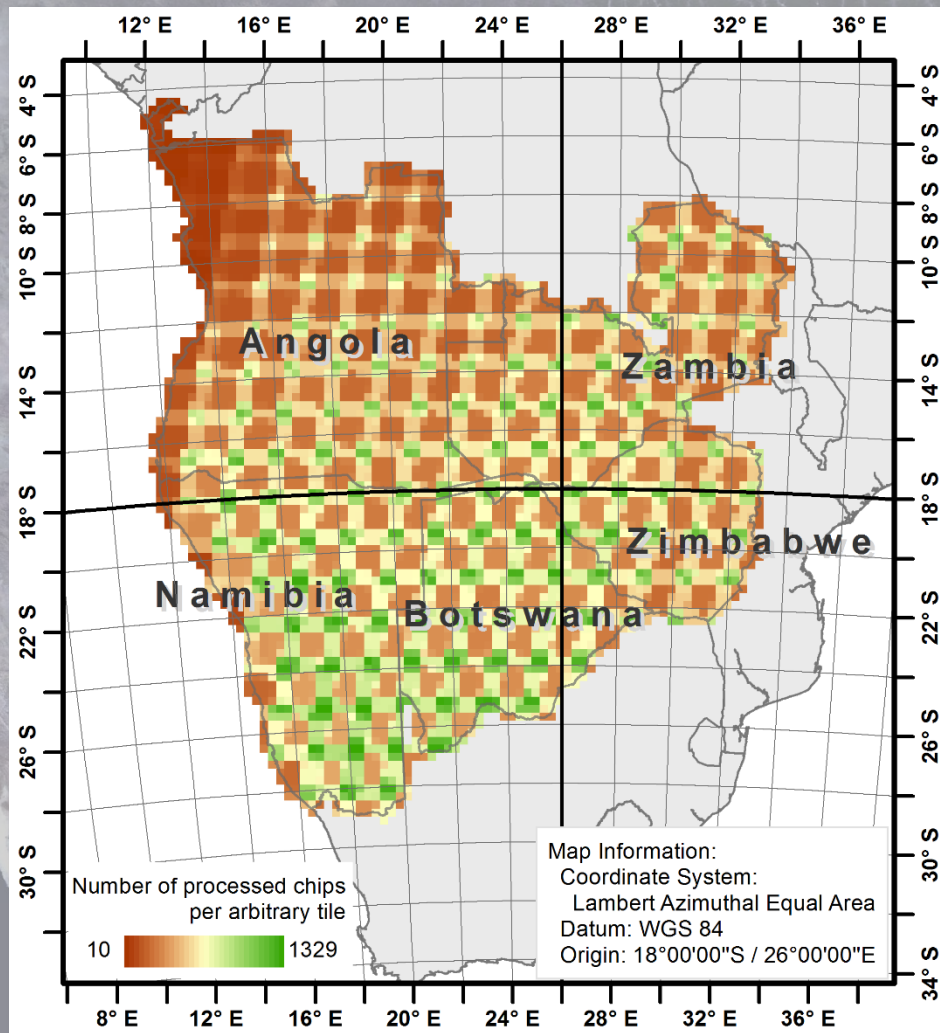
Frantz

Fmask algorithm
 (Zhu & Woodcock, 2012)
 + updates (Zhu et al., 2015)
 + modifications (Frantz et al., 2015a, Griffiths et al., 2013)





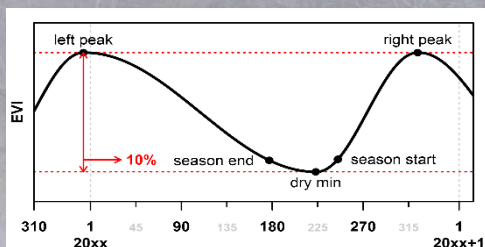
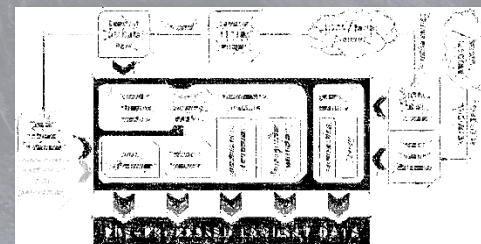
International Radiometric Landsat Pre-Processing
for Time Series Applications." In Revision.



- 29% images not fully processed → cloud coverage exceeded threshold
- 4,524 tiles
- 1,864,061 chips (i.e. tiled datasets)
- 27.18 TB processed data
- Processing time ~ 4days using 108 CPUs

LANDSAT PRE-PROCESSING

- cloud masking
- radiometric correction
- gridded data structure

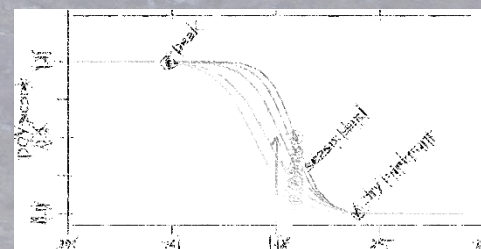


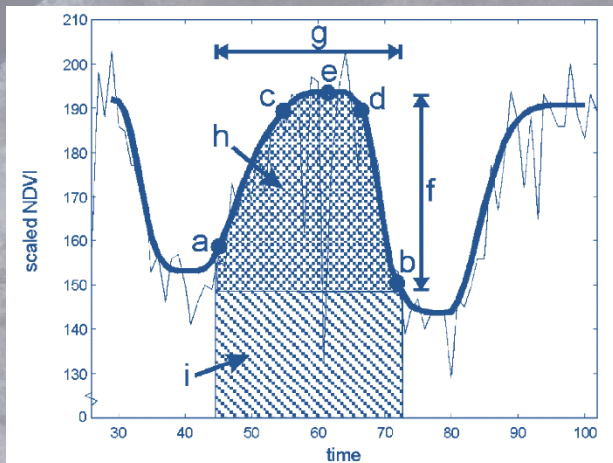
LAND SURFACE PHENOLOGY

- MODIS phenology
- Data fusion by spatial unmixing → medium resolution phenology

PIXEL-BASED COMPOSITES

- Generation of seamless large area baseline reflectance data
- Compositing guided by phenology

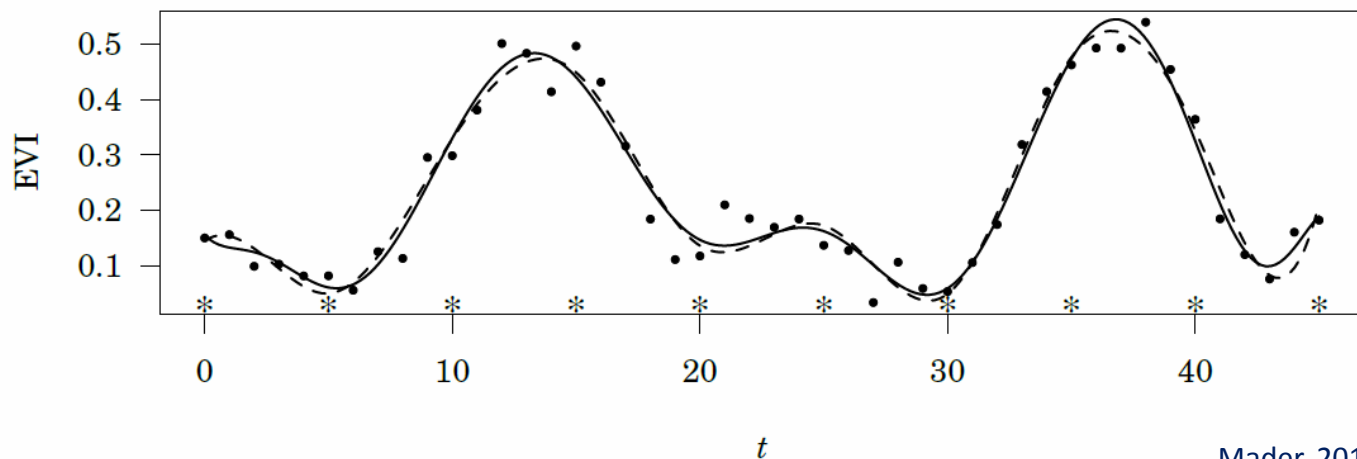




Jönsson & Eklundh 2002

Phenological descriptors are derived from high temporal resolution time series, e.g. MODIS

- Start of season (a)
- End of season (b)
- Length of season (g)
- Base value (b)
- Middle of season (e)
- Maximum of fitted data (e)
- Amplitude (f)
- Left derivative (a-c)
- Right derivative (d-b)
- Large/Total integral (i)
- Small/Green integral (h)
- Latent integral (i-h)



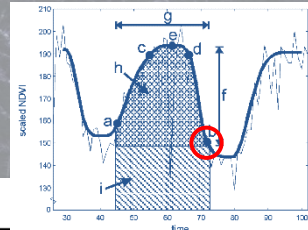
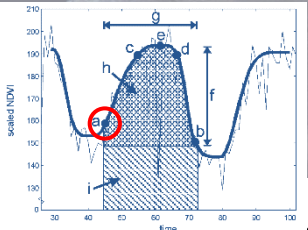
Mader, 2012

SpliTS (Spline Analysis of Time Series; Mader, 2012)

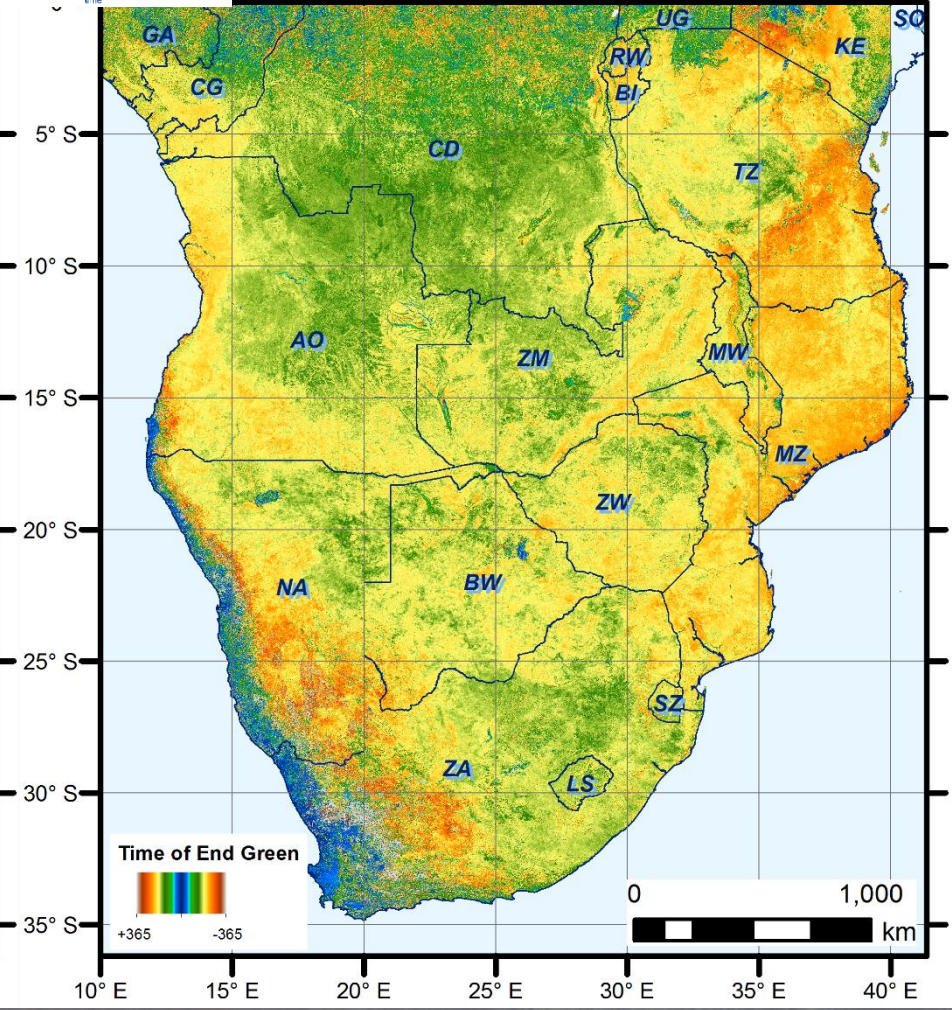
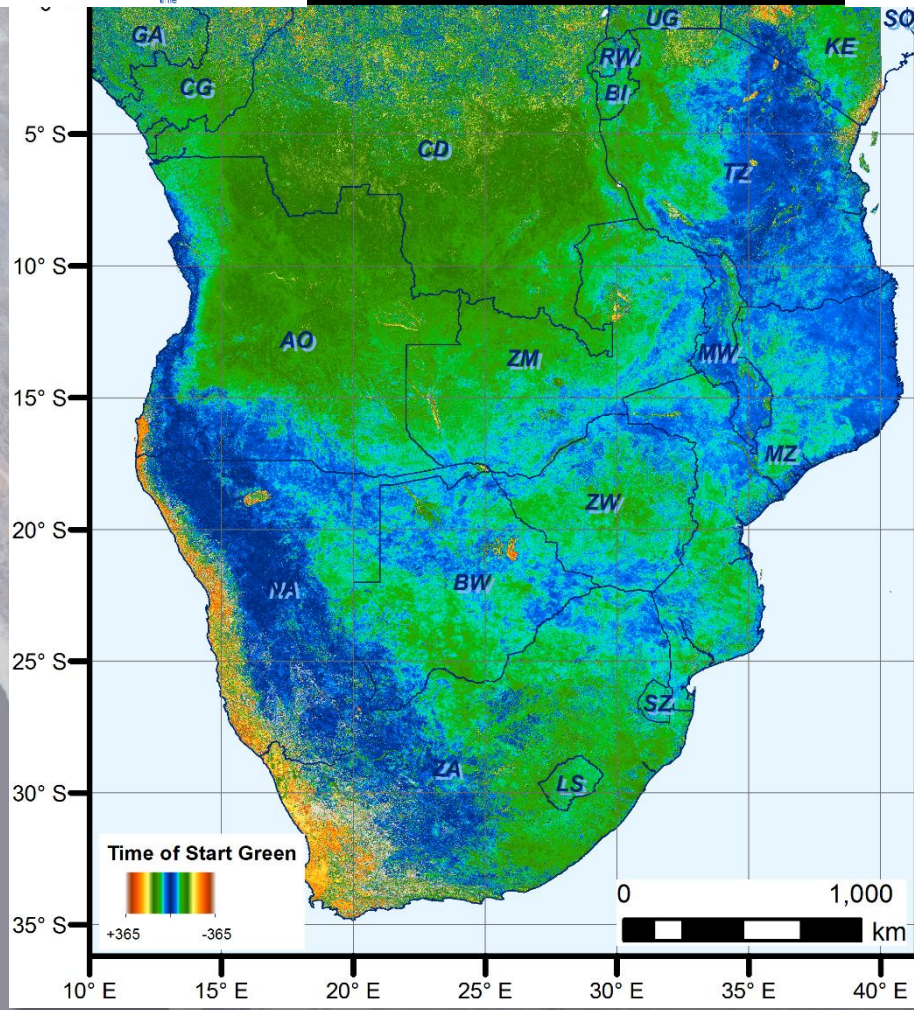
- framework for the analysis of remotely sensed time-series based on polynomial spline models
- data-driven, locally controlled fit without anticipation of a certain phenological shape
- Non-equidistant data

MODIS (Terra/Aqua) EVI time series (2000-2013) + day of composite
→ PHENOLOGICAL DESCRIPTORS

Land Surface Phenology LSP



20° E 25° E 30° E 35° E 0° E 20° E 25° E 30° E 35° E 40° E



Land Surface Phenology LSP

Data fusion via spatial unmixing

→ increase of spatial resolution by a factor of 8.3

MODIS LSP and Landsat reflectance → Landsat LSP

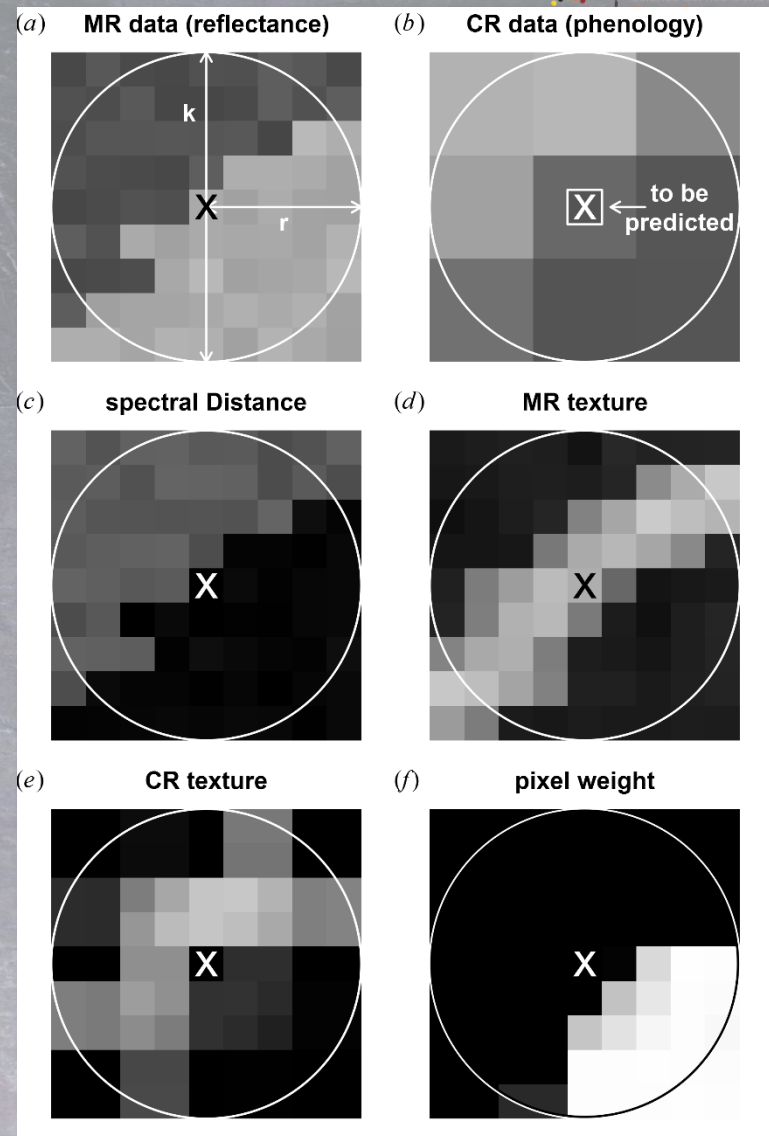
$$M_{xy,p} = \frac{\sum_{j=1}^k \sum_{i=1}^k (W'_{ji,p} C_{ji,p})}{\sum_{j=1}^k \sum_{i=1}^k W'_{ji,p}}$$

Medium resolution (MR) LSP is modelled from coarse resolution (CR) LSP

Based on the reliability of CR and MR data under different conditions, several proxies are defined:

- S_{ji} spectral distance
- T_{ji} sub-pixel heterogeneity (MR texture)
- $U_{ji,p}$ super-pixel heterogeneity (CR texture)

$$W'_{ji,p} = S'_{ji} \cdot T'_{ji} \cdot U'_{ji,p}$$



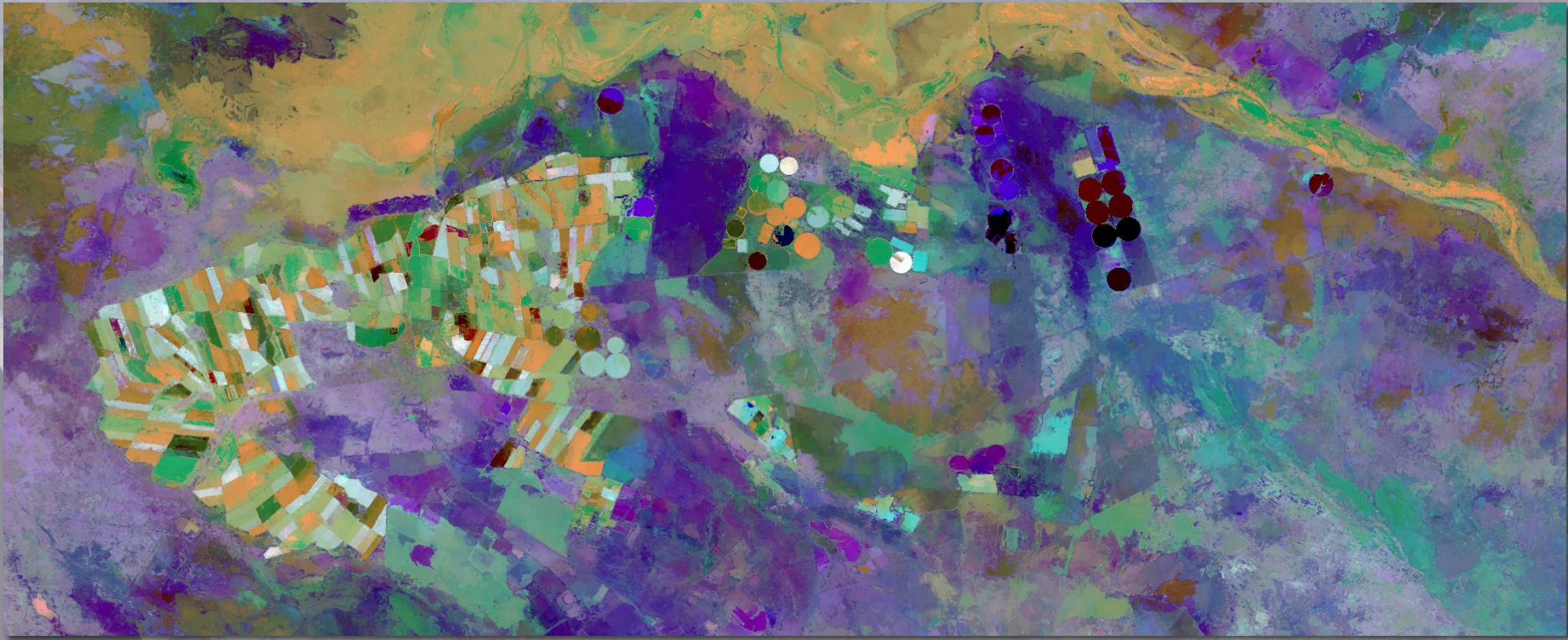
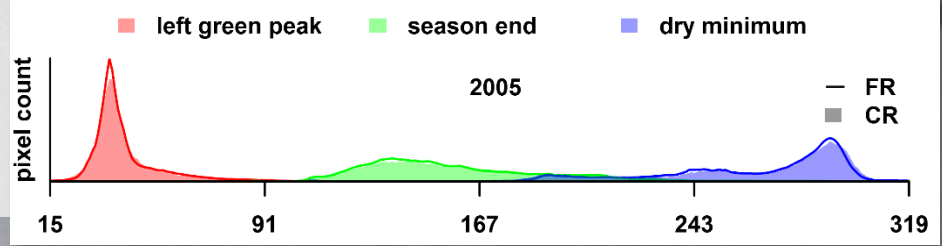
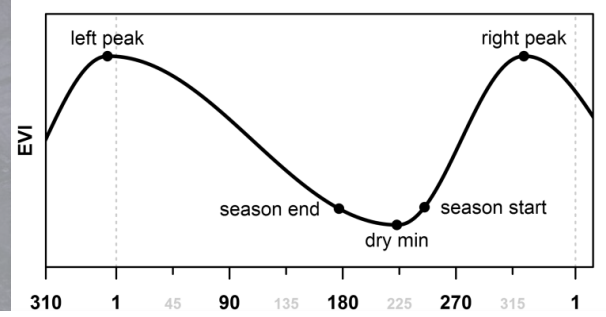
Land Surface Phenology LSP

Data fusion via spatial unmixing

→ increase of spatial resolution by a factor of 8.3

MODIS LSP and Landsat reflectance → Landsat LSP

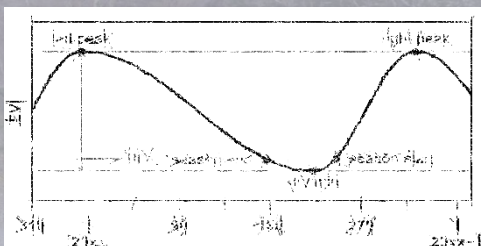
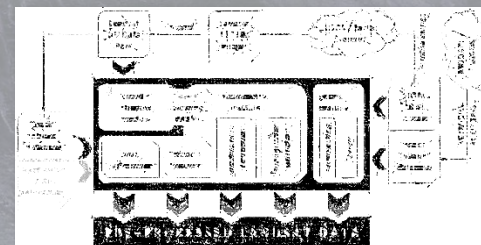
$$M_{xy,p} = \frac{\sum_{j=1}^k \sum_{i=1}^k (W'_{ji,p} C_{ji,p})}{\sum_{j=1}^k \sum_{i=1}^k W'_{ji,p}}$$



generation of wall-to-wall Landsat products

LANDSAT PRE-PROCESSING

- cloud masking
- radiometric correction
- gridded data structure

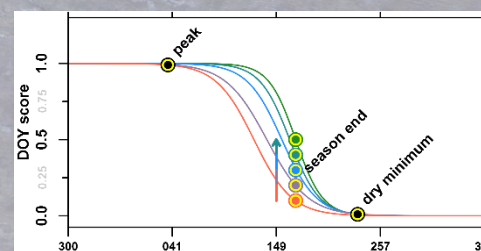


LAND SURFACE PHENOLOGY

- MODIS phenology
- Data fusion by spatial unmixing → medium resolution phenology

PIXEL-BASED COMPOSITES

- Generation of seamless large area baseline reflectance data
- Compositing guided by phenology



- Parametric weighting scheme based selection process (based on Griffiths et al., 2013)
- All Landsat images within a pre-defined time window are considered, e.g. $Y_t = 2010 \pm 2 \rightarrow 5$ years

Total score is obtained from
DOY score, **Year** score, **Cloud** score, **Haze** score

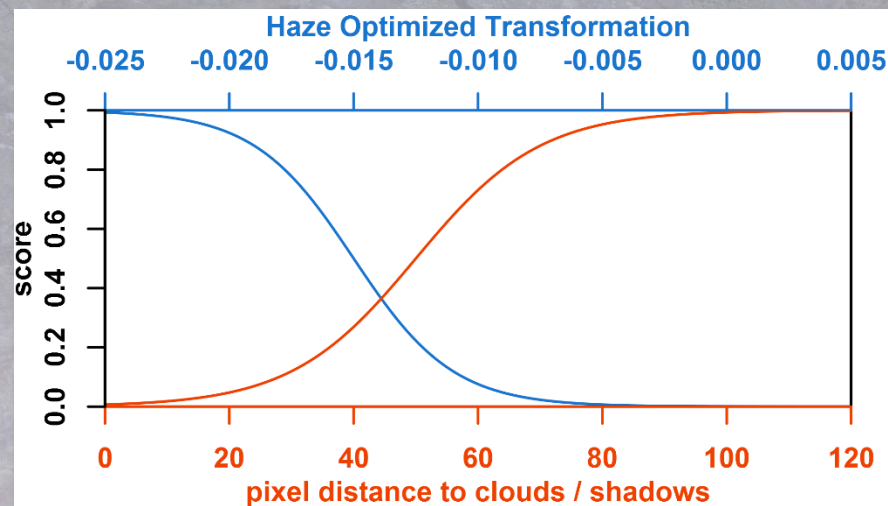
$$S_T = S_D \cdot S_Y \cdot S_C \cdot S_H$$

$$S_C = 1 / (1 + \exp(-10 / d_{req} \cdot [d_i - d_{req} / 2]))$$

d_{req} : distance after which the sky is assumed to be clear, e.g. 100px

$$S_H = 1 / (1 + \exp(500 \cdot HOT_i + 7.5))$$

HOT : Haze Optimized Transformation proxy for Haze contamination (Zhu & Woodcock, 2012)



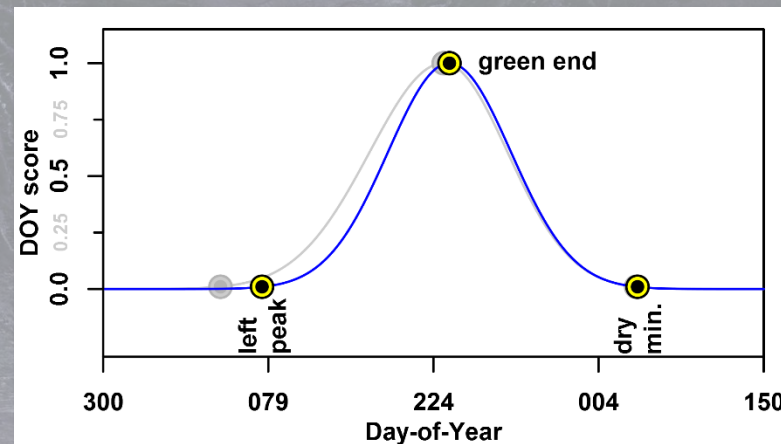
- 3 phenological descriptors are used, e.g.
 - left green peak, p_0
 - **season end**, p_1
 - dry minimum, p_2
- A Gaussian scoring function is fit to the LSP for each pixel
- The Landsat observation is scored according to its acquisition DOY D_i :

$$S_D = \begin{cases} s_l \cdot \exp(-0.5 \cdot [D_i - p_1]^2 / \sigma_l^2), & (D_i < p_1) \\ s_r \cdot \exp(-0.5 \cdot [D_i - p_1]^2 / \sigma_r^2), & (D_i \geq p_1) \end{cases}$$

- The Gaussian width is derived from the LSP and pre-defined function values at p_0, p_1, p_2 :
 - e.g. $s_0 = 0, s_1 = 1, s_2 = 0$

$$\sigma_l = [p_0 - p_1] / \sqrt{-2 \cdot \log(s_0 / s_1)}$$

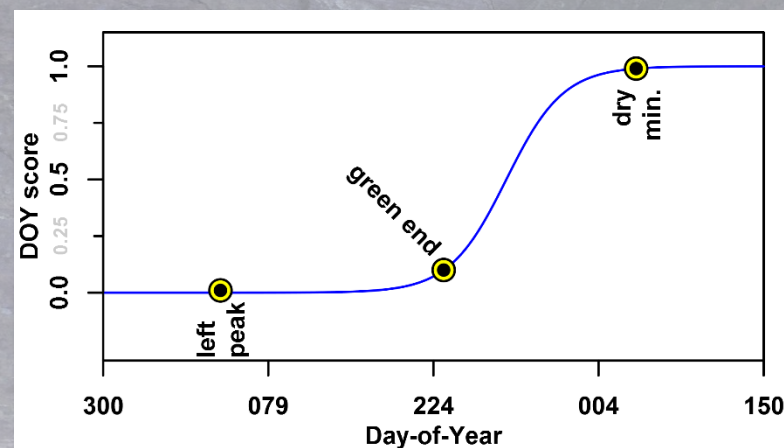
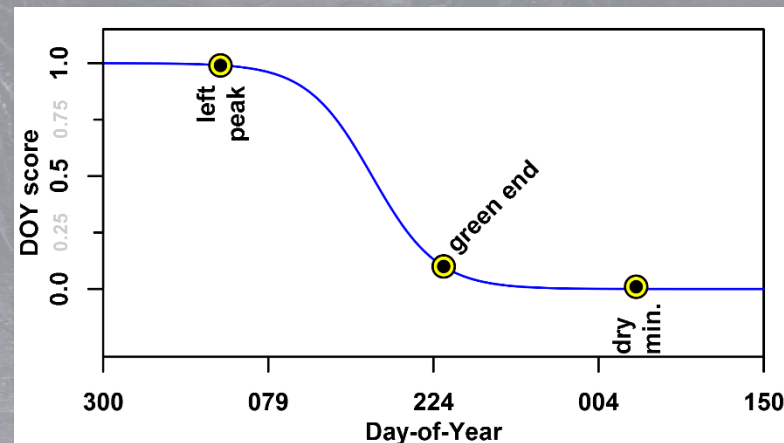
$$\sigma_r = [p_2 - p_1] / \sqrt{-2 \cdot \log(s_2 / s_1)}$$



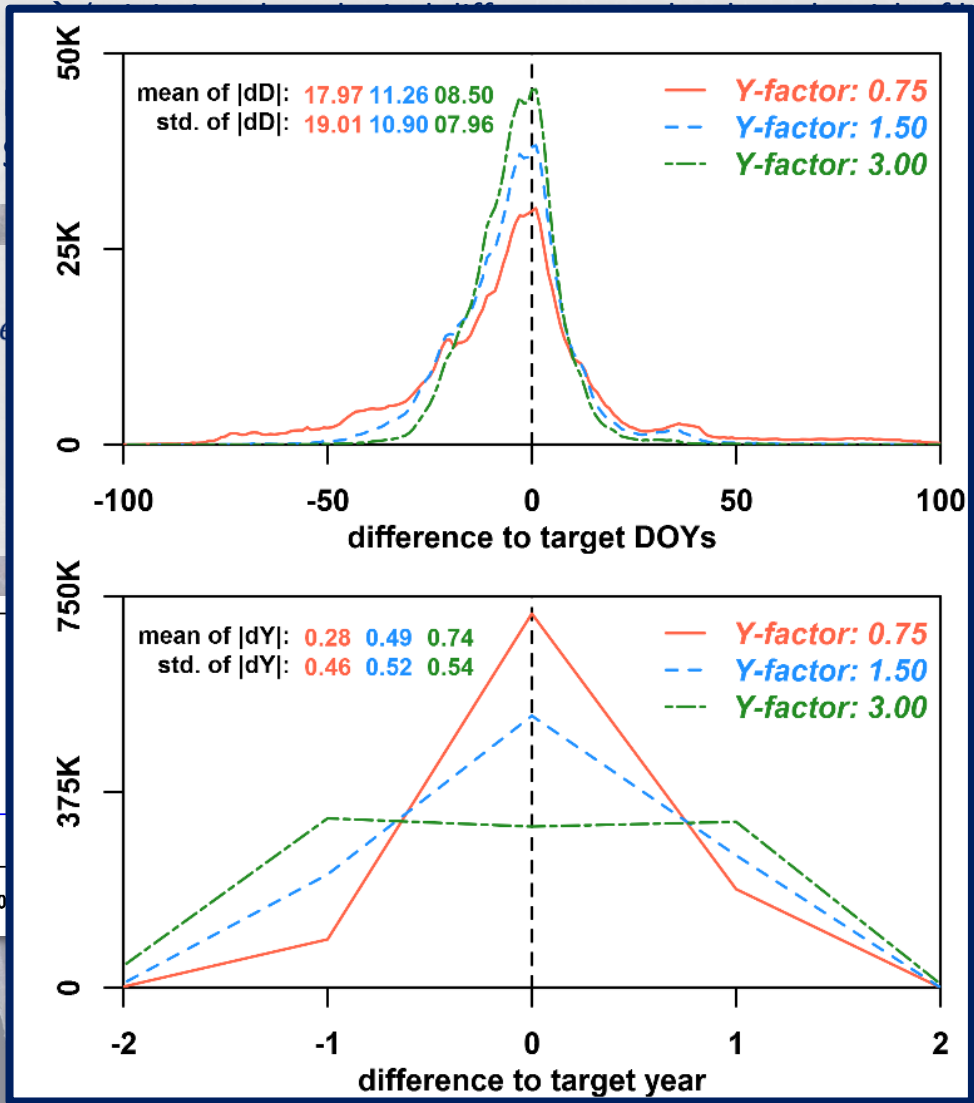
- 3 phenological descriptors are used, e.g.
 - **left green peak**, p_0
 - **season end**, p_1
 - **dry minimum**, p_2
- A logistics S-shaped scoring function is fit to the LSP for each pixel
- The Landsat observation is scored according to its acquisition DOY D_i :

$$S_D = \begin{cases} s_0 / (1 + \exp(a \cdot [D_i - p_1] + b)), & (s_0 > s_2) \\ s_2 / (1 + \exp(a \cdot [D_i - p_1] + b)), & (s_2 > s_0) \end{cases}$$

- The function parameters a and b are derived from the LSP and pre-defined function values at p_0, p_1, p_2 :
 - e.g. $s_0 = 0.99, s_1 = 0.1, s_2 = 0.01$
 - Nelder-Mead Simplex Optimization
(Nelder & Mead, 1965)



- Compositing should be mainly DOY-driven but data from the target Year should be preferred (and cover change and inter-annual variability)



with a dependency on the pixel's LSP

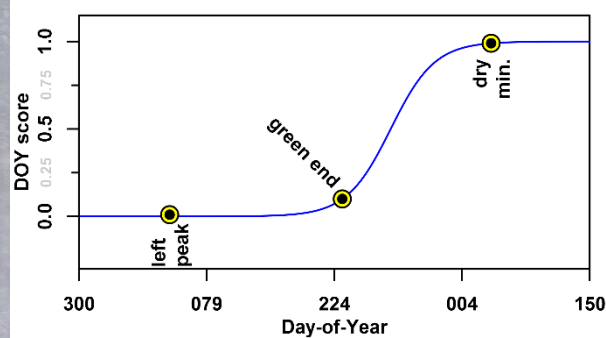
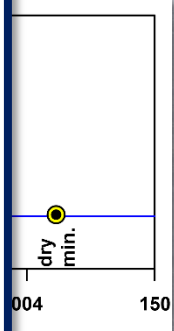
$$\exp(-0.5 \cdot [\Delta Y \cdot slice]^2 / \sigma_l^2), \quad (D_i < p_1)$$

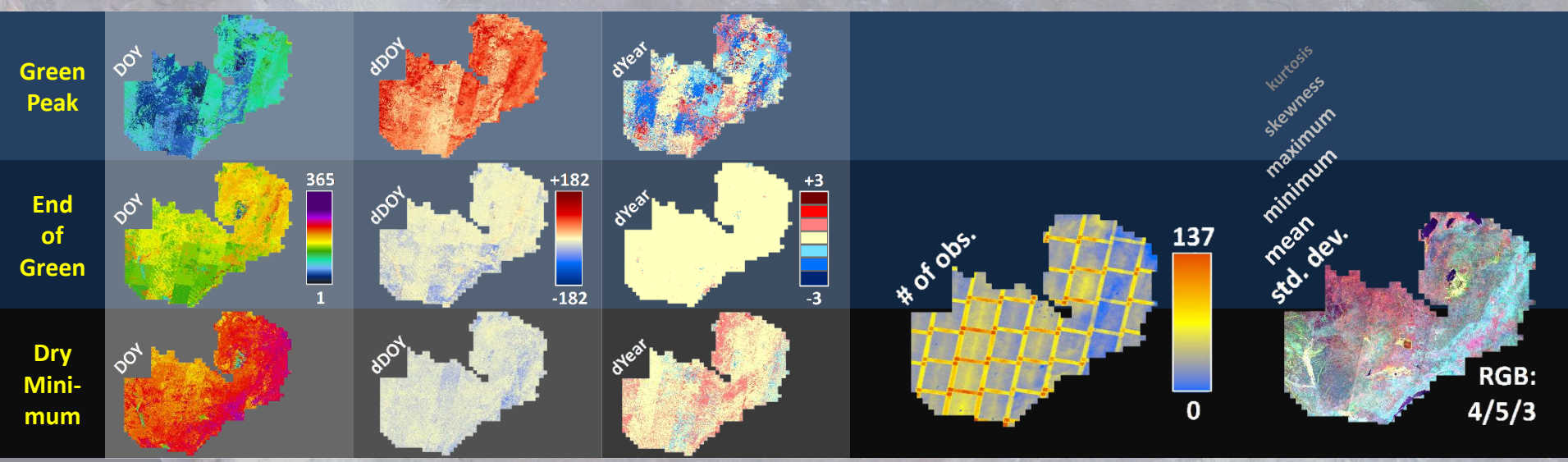
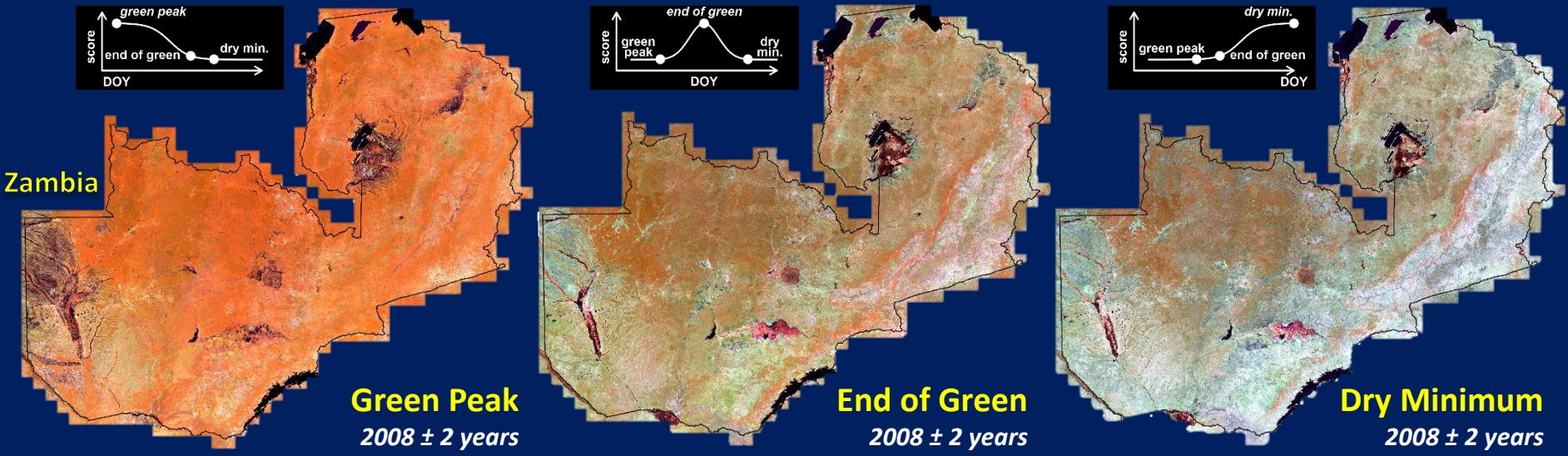
$$\exp(-0.5 \cdot [\Delta Y \cdot slice]^2 / \sigma_r^2), \quad (D_i \geq p_1)$$

$$\exp(a \cdot [p_0 + \Delta Y \cdot slice - p_1] + b), \quad (s_0 > s_2)$$

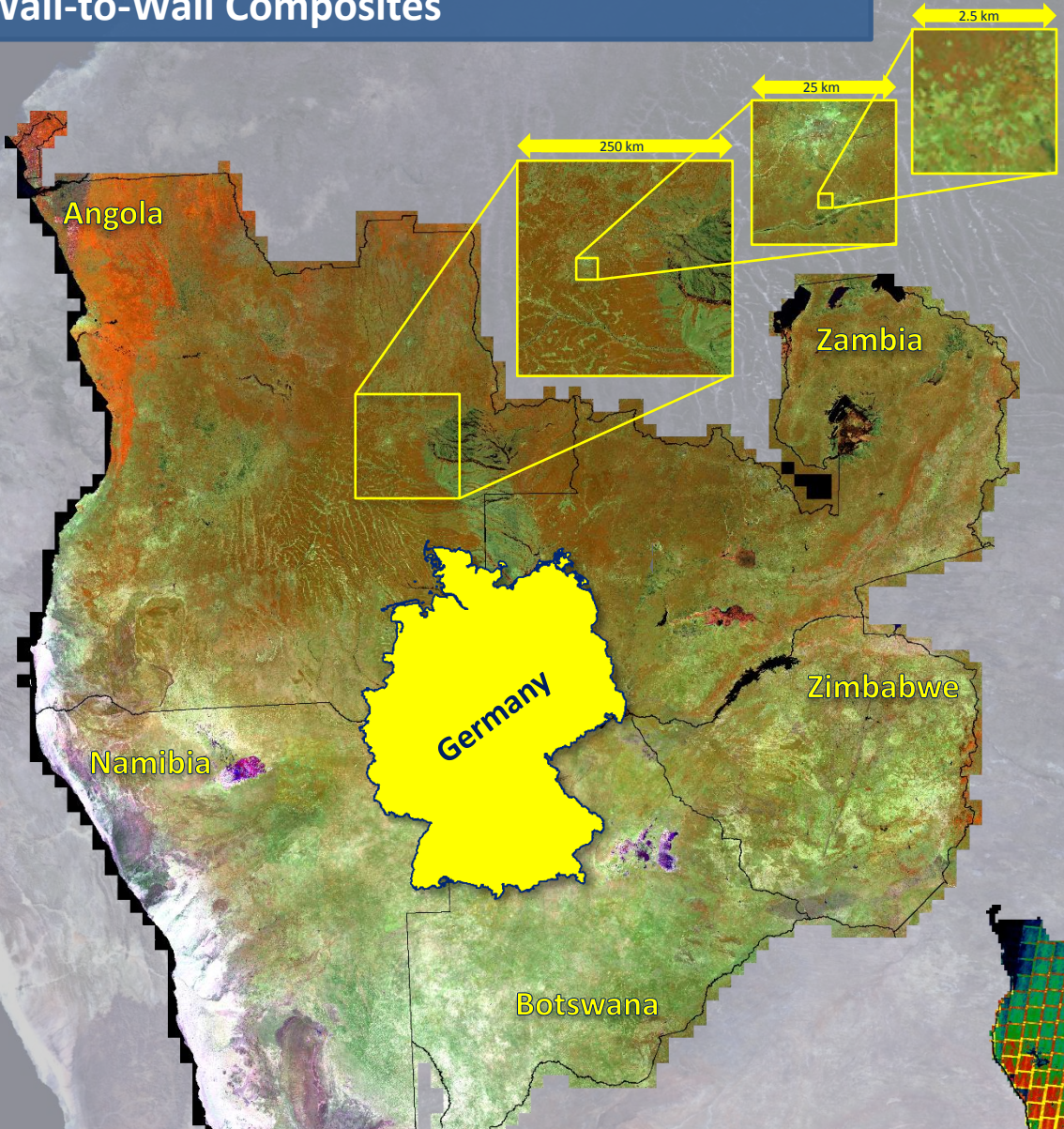
$$\exp(a \cdot [p_3 - \Delta Y \cdot slice - p_1] + b), \quad (s_2 > s_0)$$

DOY score
0.0 0.25 0.5 0.75 1.0

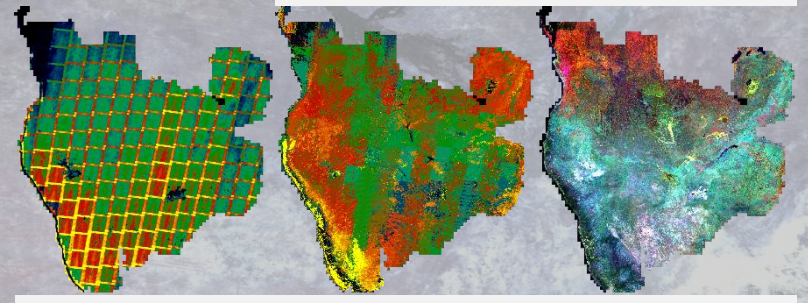
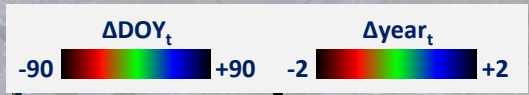
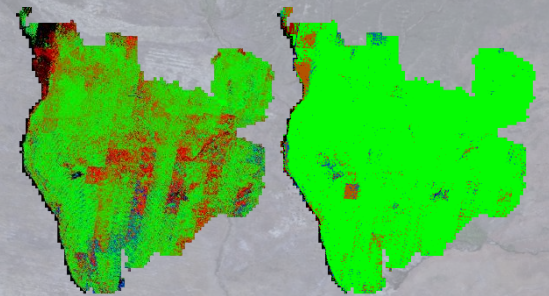




Wall-to-Wall Composites



- Composite size: 91000 x 82000 px
→ 2730 x 2460 km
- Spatial resolution: 30 m
- ~ 208 bn. observations were considered, i.e. 46 obs. / px on average
- ~ 14h processing time
- Data volume:
 - composite (6-bands): 83GB
 - composite criteria (9 bands): 125GB
 - standard deviation (6 bands): 83GB
mean, min, max, range, skewness, kurtosis
 - compositing scores (6 bands): 83GB
→ **13.9 GB / band**



- Frantz, D., A. Röder, et al. "An operational radiometric Landsat pre-processing framework for large area time series applications." In Revision.
- Frantz, D., A. Röder, et al. (2015). "On the derivation of a spatially distributed aerosol climatology for its incorporation in a radiometric Landsat pre-processing framework." *Remote Sensing Letters* 6(8): 647-656.
- Frantz, D., A. Röder, et al. (2015). "Enhancing the Detectability of Clouds and Their Shadows in Multitemporal Dryland Landsat Imagery: Extending Fmask." *IEEE Geoscience and Remote Sensing Letters* 12(6): 1242-1246.
- Griffiths, P., S. van der Linden, et al. (2013). "A Pixel-Based Landsat Compositing Algorithm for Large Area Land Cover Mapping." *IEEE Journal of Selected Topics in Applied Earth Observations and Remote Sensing* 6(5): 2088-2101.
- Hill, J. (1993). High precision land cover mapping from multitemporal earth observation satellite data: the Ardèche experiment. Faculty of Geography/Geosciences, Trier University. Ph.D.: 121.
- Hill, J. and B. Sturm (1991). "Radiometric correction of multitemporal Thematic Mapper data for use in agricultural land-cover classification and vegetation monitoring." *International Journal of Remote Sensing* 12(7): 1471-1491.
- Jonsson, P. and L. Eklundh (2002). "Seasonality extraction by function fitting to time-series of satellite sensor data." *IEEE Transactions on Geoscience and Remote Sensing* 40(8): 1824-1832.
- Mader, S. (2012). A Framework for the Phenological Analysis of Hypertemporal Remote Sensing Data Based on Polynomial Spline Models. *Geographie/Geowissenschaften, Trier University*. Dr. rer. nat.: 101.
- Nelder, J. A. and R. Mead (1965). "A Simplex Method for Function Minimization." *The Computer Journal* 7(4): 308-313.
- Röder, A., T. Kuemmerle, et al. (2005). "Extension of retrospective datasets using multiple sensors. An approach to radiometric intercalibration of Landsat TM and MSS data." *Remote Sensing of Environment* 95(2): 195-210.
- Tanré, D., C. Deroo, et al. (1990). "Description of a computer code to simulate the satellite signal in the solar spectrum: the 5S code." *International Journal of Remote Sensing* 11(4): 659-668.
- Zhu, Z., S. Wang, et al. (2015). "Improvement and expansion of the Fmask algorithm: cloud, cloud shadow, and snow detection for Landsats 4–7, 8, and Sentinel 2 images." *Remote Sensing of Environment* 159(0): 269-277.
- Zhu, Z. and C. E. Woodcock (2012). "Object-based cloud and cloud shadow detection in Landsat imagery." *Remote Sensing of Environment* 118(0): 83-94.

Thank you for your attention!

Questions? / Fragen?